Analysis of ALTAIR 1998 meteor radar data

J. Zinn,[1] S. Close,[2] P. L. Colestock,[1] A. MacDonell,[3] and R. Loveland[1]

Received 21 June 2010; revised 21 January 2011; accepted 25 January 2011; published 16 April 2011.

[1] We describe a new analysis of a set of 32 UHF meteor radar traces recorded with the 422 MHz Advanced Research Project Agency Long-Range Tracking and Identification Radar facility in November 1998. Emphasis is on the absolute velocity measurements and inferences that can be drawn from them regarding the meteoroid masses and mass densities. We find that the 3-D velocity versus altitude data can be fitted as quadratic functions of the path integrals of the atmospheric densities versus distance, and deceleration rates derived from those fits all show the expected behavior of increasing with decreasing altitude. We also describe a computer model of the coupled processes of collisional heating, radiative cooling, evaporative cooling and ablation, and deceleration for meteoroids composed of defined mixtures of mineral constituents. For each of the cases in the data set, we ran the model starting with the measured initial velocity and trajectory inclination and with various trial values of the quantity $m\rho_s^2$ (initial mass times mass density squared) and then compared the computed deceleration versus altitude curves versus the measured ones. In this way we arrived at the best fit values of the $m\rho_s^2$ for each of the measured traces. Then further, assuming various trial values of the density ρ_s, we compared the computed mass versus altitude curves with similar curves for the same set of meteoroids determined previously from the measured radar cross sections and an electrostatic scattering model. In this way we arrived at estimates of the best fit mass densities ρ_s for each of the cases.

Citation: Zinn, J., S. Close, P. L. Colestock, A. MacDonell, and R. Loveland (2011), Analysis of ALTAIR 1998 meteor radar data, *J. Geophys. Res.*, *116*, A04312, doi:10.1029/2010JA015838.

1. Introduction

[2] This paper describes a new analysis of a set of 422 MHz meteor scatter radar data recorded with the Advanced Research Project Agency Long-Range Tracking and Identification Radar (ALTAIR) High-Power-Large-Aperture radar facility at Kwajalein Atoll on 18 November 1998. The exceptional accuracy/precision of the ALTAIR tracking data allows us to determine quite accurate meteoroid trajectories, 3-D velocities and deceleration rates. The measurements and velocity/deceleration data analysis are described in sections 2 and 3. The main point of this paper is to use these deceleration rate data, together with results from a computer model, to determine values of the quantities $m\rho_s^2$ (the meteoroid mass times its material density squared); and further, by combining these $m\rho_s^2$ values with mass estimates for the same set of meteoroids determined separately from measured radar scattering cross sections, to arrive at estimates of the mass densities ρ_s.

[3] The computer model, described in section 4 and Appendix A, treats the simultaneous processes of meteoroid heating through air molecule collisions, blackbody radiation emission, evaporation, sputtering, and deceleration for meteoroids of specified assumed initial mixtures of mineral constituents. The model assumes in each case that the meteors are spherical, and remain so without fragmenting. It includes an imbedded table of atmospheric mass densities versus altitude and data on (1) vapor pressure versus temperature, (2) heat of sublimation, (3) vapor molecular weight, and (4) melting point for each of the assumed constituent species. Other inputs to the model include, for each individual case, (1) the initial velocity and trajectory inclination (i.e., at the top of the atmosphere) and (2) trial values of the initial $m\rho_s^2$ (i.e., values before entering the atmosphere).

[4] The data include 32 individual traces, where almost all the meteoroids appear to be in the mass range 10^{-6} to 10^{-3} grams, and the altitudes are such that air molecule collision mean free paths are much larger than the meteoroid dimensions. Thus air molecule collisions with the meteoroid can be regarded as isolated events, and fluid dynamic effects do not apply (large Knudsen number). In our data analysis we fit the reduced data on velocities versus altitude and trajectory inclination as least squares quadratic functions of the path-integrated air column densities, using tabular data on air densities versus altitude. We then compute the corresponding deceleration rates. We find, as expected, that for all the traces the deceleration rates increase with decreasing altitude.

[5] The model equations and variables are listed in Appendix A.

[1]Los Alamos National Laboratory, Los Alamos, New Mexico, USA.
[2]Department of Aeronautics and Astronautics, Stanford University, Stanford, California, USA.
[3]Department of Astronomy, Boston University, Boston, Massachusetts, USA.

0148-0227/11/2010JA015838

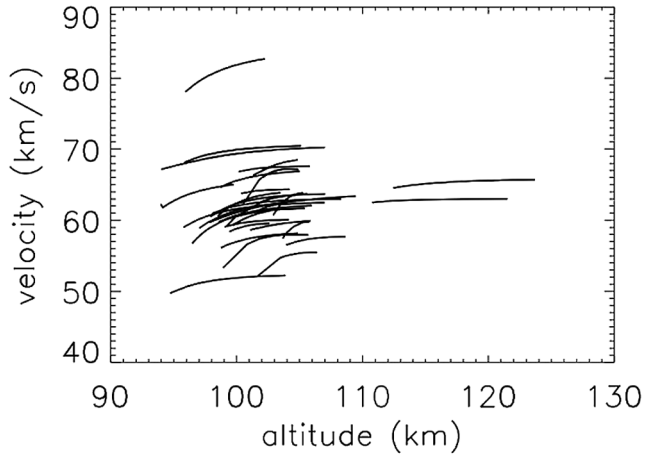

Figure 1. Composite plot of the fitted velocities versus altitude for the 32 cases, from the least squares quadratic fits of the measured velocities versus Q. (Note that one meteor streak appears to be hyperbolic, with a velocity exceeding 72.8 km/s. We will perform orbital analysis on this streak in the future to confirm this result.)

[6] Appendix B describes a quasi-analytic solution of the ablation equations for a 1-component meteoroid, using the steady state approximation. It shows that at the lowest altitudes the meteoroid temperatures are determined mainly by an equilibrium between collisional heating and evaporative cooling. And the ablation coefficients tend to approach a common value equal to the vapor molecular weight divided by twice the heat of vaporization, and independent of the initial velocity.

2. Experiment

[7] The ALTAIR High-Power-Large-Aperture radar facility is located on the Kwajalein Atoll (9°N, 167°E) in the Republic of the Marshall Islands. ALTAIR has a 43 m diameter mechanically steered parabolic dish, and simultaneously transmits a peak power of 6 MW at two frequencies (VHF-160 MHz, and UHF-422 MHz) [*Close et al.*, 2000, 2002a, 2002b, 2002c, 2004]. The radar characteristics are described in detail in those references. It is particularly suited for precise measurements of small targets at long ranges. Extensive measurements going back to 1983 show stable RMS tracking accuracies of ±15 millidegrees in angle and ±6 m in range. In the present paper we discuss a UHF data set consisting of 32 meteoroid traces obtained on 18 November 1998. The radar sample window encompassed slant ranges corresponding to heights mostly between 90 to 110 km. 150 μs pulsed waveforms were used, with a range sample spacing corresponding to about 7.5 m. The instantaneous meteor three-dimensional positions were determined from the monopulse range and angular measurements, and the velocities were determined by fitting the head echo range versus time data to a third-order polynomial [*Close et al.*, 2002b].

3. Data Analysis

[8] For each of the 32 meteor traces (using the tabulated altitudes, velocities and vertical velocity components versus time) we begin by performing a quadratic least squares fit to the velocities versus the air path traversed (Q), where

$$Q \equiv \int_z^\infty \rho \, ds, \tag{1}$$

ρ is the local air density and ds is the element of distance along the meteoroid path to the altitude z. The ρ's were taken from MSIS-E-90 (NASA-GSFC web site http://ccmc.gsfc.nasa.gov/cgi-bin/modelweb/models/vitmo_model.cgi), and the Q integrals were evaluated for each point along each trace using the measured trajectory inclination angles. (We will regard these atmospheric density data as given, and note that they are probably more accurately determined than are the meteor masses or mass densities that we will derive from the radar data.) Then from the Q derivative of this fitted quadratic velocity versus Q function we compute the corresponding deceleration rates as functions of z. Figure 1 is a composite plot of the fitted velocities versus altitude for the 32 traces. It will be noted that they all show velocities decreasing with decreasing altitude, and all of them show some downward curvature. Likewise, the deceleration rates increase with decreasing altitude, as they should. Figure 2 is a composite plot of the decelerations (negative accelerations) versus altitude for the 32 traces, derived from the velocity fits.

[9] We note that in four of the cases the initial value of dv/dt has come out to be positive, presumably due to inaccuracies in the velocity data. (Of these four, three were unusually short traces less than 3 km long.) These cases will be discarded, as well as one other case where the fitted deceleration curve is abnormal. Despite the problems with these five cases, this fitting procedure seems to give generally reasonable results. A simple dependency of velocities on Q is of course expected on physical grounds. And in all 32 cases the deceleration rates increase with decreasing altitude, as they should. Moreover, in all but one case the curvature of the dv/dt versus z plot is downward, as it should be (i.e., $d^2(dv/dt)/dz^2$) is negative.) (The signs of $d(dv/dt)/dz$ and $d^2(dv/dt)/dz^2$ can be deduced

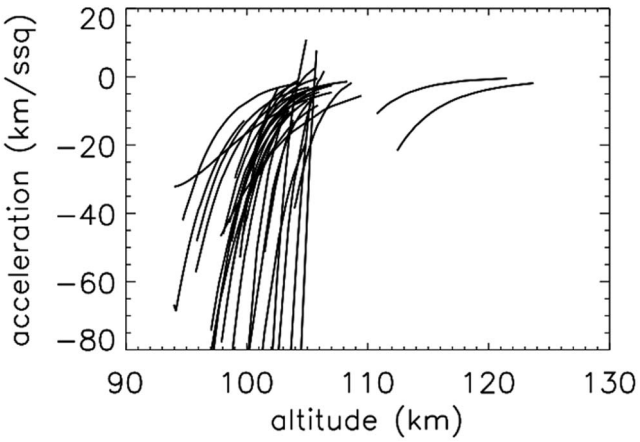

Figure 2. Composite plot of the accelerations versus altitude for the 32 cases as derived from the quadratic fits to the velocities.

from equations (3) and (4), together with an expression for the variation of ρ with z.)

[10] In this paper we hope to show that measurements of velocity and deceleration rates can lead to believable values of the meteoroid masses (or more precisely the $m\rho_s^2$ or ballistic parameters. Values of the mass density ρ_s must still be assumed.)

[11] In our analysis we will assume that the meteoroids are spherical. Then the energy flux on the meteor surface due to air molecule collisions is $\pi r^2 \rho v^3/2$, where r and v are the meteor radius and velocity, and ρ is the local air density. Consistent with other authors [e.g., *Pecina and Ceplecha*, 1983; *Opik*, 1958; *Bronshten*, 1983; *Ceplecha et al.*, 1998] we will write the meteor mass loss rate as

$$dm/dt = -\pi r^2 \rho v^3 \sigma, \tag{2}$$

where m is the mass and σ is the "ablation coefficient." The rate of deceleration of the meteoroid is

$$dv/dt = -\pi r^2 \rho v^2/m. \tag{3}$$

Combining equations (1) and (2) we obtain

$$dm/m = \sigma \; v \; dv. \tag{4}$$

If we make the convenient (but not necessarily valid) assumption that σ is constant, then equation (3) can be integrated, giving

$$\ln(m/m_1) = (\sigma/2)\left(v^2 - v_1^2\right), \tag{5}$$

where m_1 and v_1 are the initial values of m and v along a given meteor radar trace. The constant σ assumption would be appropriate if, for instance, the meteoroid mass loss was dominated by "sputtering."

[12] In an alternative model [e.g., *Vondrak et al.*, 2008; *Janches et al.*, 2009; *Lebedinets*, 1973], the mass loss is dominated by thermal evaporation of the meteor constituents. The instantaneous evaporation rate for each constituent is determined by the instantaneous temperature. In section 4 we describe our own numerical model of these coupled processes, which is similar in many respects to the Vondrak et al. model.

4. Numerical Model

[13] The consensus of most current theoretical studies of the ablation and slowing down of small meteors in the atmosphere [*Lebedinets*, 1973; *Janches et al.*, 2009; *Vondrak et al.*, 2008] is that (1) very rapid heating occurs due to collisions with air molecules, moderated by energy losses due to blackbody emission from the surface and due to evaporation. (2) The heating leads to vaporization of meteor constituents (generally preceded by melting). (3) Some sputtering occurs, in addition to the vaporization. (4) The air molecule collisions also lead to deceleration. (5) With very small meteoroids the rate of internal heat conduction is sufficient to maintain a uniform temperature distribution within the meteoroid body. (6) Meteoroids are composed of mixtures of chemical constituents, and each will vaporize at its own rate.

[14] In the present model we further assume that the meteor is spherical, and that after melting it does not disintegrate.

[15] The rate of heating through air molecule collisions is

$$(dH/dt)_{coll} = \pi r^2 \rho v^3/2,$$

where r is the instantaneous meteoroid radius, v its instantaneous velocity, and ρ the local air density, and it is assumed that all the energy of a collision is transferred to the meteoroid. The rate of loss of energy by blackbody emission is

$$(dH/dt)_{rad} = -4\pi r^2 \sigma_{SB} T^4,$$

where σ_{SB} is the Stephan-Boltzmann constant and T is the instantaneous temperature. The vapor pressure of the *i*th chemical constituent of the meteor is given by the Claussius-Clapeyron equation

$$P_{vap(i)} = A_i \exp(-C_i/T), \tag{6}$$

where A_i and C_i are constants characteristic of the particular constituent. The evaporative flux of each constituent from the surface is given by the Langmuir relation

$$F_{evap(i)} = C_{flx} \, P_{vap(i)} / \left(\mu_{vap(i)} T\right)^{1/2} \left(\text{molecules/cm}^2\text{s}\right), \tag{7}$$

[*Taylor and Langmuir*, 1933], where $\mu_{vap(i)}$ is the molecular weight of the vapor. If $P_{vap(i)}$ is in dynes/cm^2 and $\mu_{vap(i)}$ is in grams, then the constant C_{flx} is equal to 3.40×10^7. Then the rate of energy loss from the meteoroid surface due to evaporation of each constituent is

$$(dH/dt)_{evap(i)} = -4\pi r^2 \Delta H_{sblm(i)} F_{evap(i)}, \tag{8}$$

where $\Delta H_{sblm(i)}$ is the heat of sublimation (erg/molecule). Then the rate of change of the meteoroid temperature is

$$dT/dt = \left[(dH/dt)_{coll} + (dH/dt)_{rad} + \sum\nolimits_{(i=1,N)} (dH/dt)_{evap(i)}\right]/C_p, \tag{9}$$

where C_p is the specific heat. In equation (9) it is assumed that each constituent vaporizes at a rate independent of the other constituents, as long as that constituent is still present (i.e., has not totally evaporated). Values of the parameters $\Delta H_{sblm(i)}$, A_i, C_i, $\mu_{vap(i)}$ and melting point for several likely meteor constituents are listed in Table 1, below.

[16] Table 1 shows the physicochemical parameters that we have assumed for several possible meteoroid constituents, including A, C, ΔH_{sblm}, and some references. In most cases the references do not give the quantities A, C and ΔH_{sblm} directly, and in those cases we have had to calculate those quantities by fitting equation (6) to data on vapor pressures measured at two or more temperatures, and assuming that ΔH_{sblm} is equal to the Boltzmann constant k_B times C_i. The references listed in Table 1 are mostly sources of vapor pressure and/or boiling point data.

[17] The rate of loss of mass from the meteoroid due to evaporation, is

$$(dm/dt)_{evap} = -4\pi r^2 \sum\nolimits_{(i=1,N)} \left(\mu_{vap(i)} \; F_{evap(i)}\right). \tag{10}$$

Table 1. Physicochemical Parameters for Meteor Constituents and References

Constituent	ΔH_{sblm} (erg/molec)	A (dyne/cm^2)	C(K)	μ_{vap} (g)	Melting Point (K)	References
Fe (iron metal)	6.62e-12	5.06e + 12	4.836e + 4	9.30e-23	1811	[*Ferguson et al.*, 2004]
C (graphite)	1.495e-11	9.74e + 15	1.006e + 5	3.99e-23	-	[*Brewer et al.*, 1948; *Clarke and Fox*, 1969]
SiO_2	9.64e-12	4.16e + 11	6.99e + 4	9.97e-23	1923	[*Wickramasinghe and Swamy*, 1968]
MgO	8.65e-12	9.16e + 14	6.27e + 4	6.64e-23	3073	[*Brewer and Porter*, 1954]
FeO	1.03e-11	1.01e + 16	7.47e + 4	1.20e-22	1653	[*Akopov*, 1999; *Fabian*, 1993; *Patnaik*, 2002]

There will also be some mass loss due to sputtering, given by

$$(dm/dt)_{sputt} = \pi r^2 \rho v^3 \sigma_{sputt},$$

where σ_{sputt} is the ablation coefficient associated with sputtering (units of s^2/cm^2). The meteoroid radius r is related to the mass m by $r = (3m/4\pi\rho_s)^{1/3}$, where ρ_s is the mass density of the solid body.

[18] Finally, the rate of deceleration of the meteoroid is given by equation (3). We have developed our own computer model that incorporates the above processes in the form of a set of ordinary differential equations expressing the rates of change of meteoroid mass, velocity, radius, temperature, etc. as functions of time (code name "meteorstpg_hialt9.f" version of 22 July 2010). The input composition can be either a pure compound or a mixture of compounds. The differential equations are detailed in Appendix A. This model appears to be very similar to the one described by *Vondrak et al.* [2008].

[19] Some key questions are, of course (1) What is the meteor composition? (2) What is its mass and mass density? (3) Does the meteoroid actually remain intact after it melts? and (4) What is the contribution of sputtering to the total ablation coefficient?

5. Some Numerical Results

5.1. Determination of the $m\rho_s^2$

[20] Figures 3a and 3b show comparisons, for two typical traces, of computed versus measured decelerations versus altitude. For inputs to the computations for each trace we take (1) the measured initial velocity and initial altitude; (2) the measured trajectory inclination angle; (3) an assumed initial (top-of-atmosphere) value of $m\rho_s^2$, which is shown on each plot; (4) an assumed initial composition, namely, an equimolar mixture of SiO_2, FeO and MgO (which corresponds roughly to the expected decomposition products of olivine, a mineral that is commonly found in stony meteorites); (5) an assumed energy for sputtering, E* = 15 eV per molecule, giving a constant sputtering contribution of 2.1×10^{-12} s^2/cm^2 to the total ablation coefficients; and (6) a mass density ρ_s of 1.0 g/cm^3 (see next paragraph). The assumed initial $m\rho_s^2$ value is varied to produce the best fit to the experimental data. With these assumptions Figures 3a and 3b show good agreement between the computed results and the data. In all, we found satisfactory agreement in 20 of the 32 cases.

[21] We also ran computations with other assumed mass densities (ρ_s) and sputtering energies (E*), although the results will not be shown here. From comparisons of the results with Figures 3a and 3b we found that the computed deceleration rates did not depend at all on the assumed density ρ_s. This is to be expected, since the initial meteoroid mass is equal to the input $m\rho_s^2$ divided by ρ_s^2, and the separate dependencies of the acceleration rates on m and ρ_s are always connected through the $m\rho_s^2$.

[22] We also found that without the assumed relatively large sputtering contribution to the ablation coefficients the agreement with the data was less good than the extent of agreement shown in Figures 3a and 3b.

5.2. Determination of m and ρ_s Separately

[23] Although the computed deceleration values are independent of the separate values of m and ρ_s (once the initial value of the product $m\rho_s^2$ is prescribed), the time-varying $m\rho_s^2$ do depend on ρ_s, and the mass m is of course equal to $m\rho_s^2/\rho_s^2$. Because of this it is possible to arrive at rough estimates of both m and ρ_s separately, using the measured values of decelerations and radar cross sections in combination, and using m values derived using the Close et al. electrostatic scattering model [*Close et al.*, 2004, 2005] together with the fitted $m\rho_s^2$ values obtained with the abla-

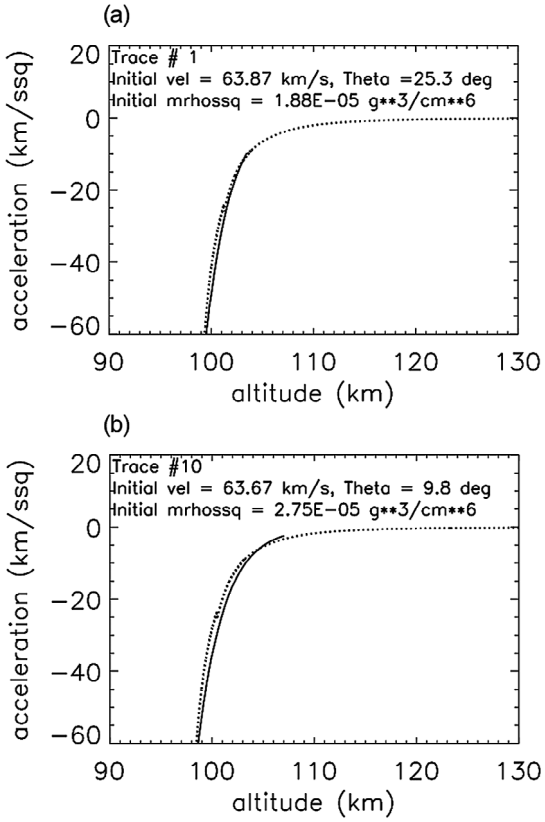

Figure 3. (a and b) In each of these plots the solid curve is the acceleration derived from the data fit, and the dotted curve is the one computed with the model (with inputs described in the text).

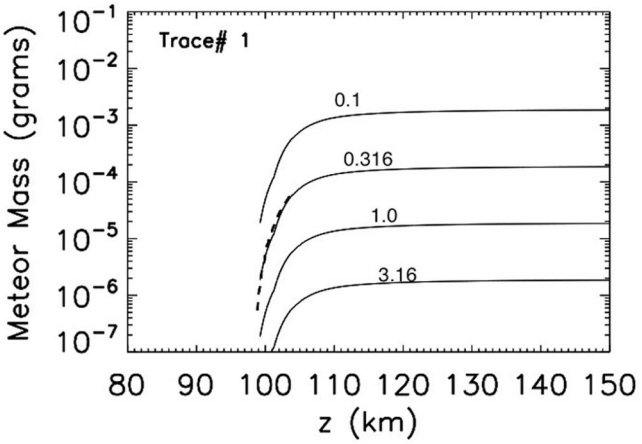

Figure 4a. Here the solid curves are the inertial masses (for trace #1) computed with the numerical model, using the best fit value of $m\rho_s^2$ together with four different assumed values of the meteor density ρ_s, namely (from top to bottom), 0.1, 0.316, 1.0, and 3.16 g/cm^3. The dashed curve is the "mass1" (mass determined from the measured cross sections together with the electrostatic scattering model).

tion and deceleration model. The electrostatic scattering model will be discussed briefly in Appendix C. Figures 4a and 4b show two examples of such attempts to determine both m and ρ_s from the experimentally determined $m\rho_s^2$ and "mass1" (mass from the radar cross sections). In Figure 4a, representing trace #1, the four solid curves are the computed inertial mass values versus altitude derived from the best fit $m\rho_s^2$ (from Figure 3a) assuming four different values of ρ_s, namely, 0.1, 0.316, 1.0 and 3.16 g/cm^3, while the dashed curve is mass1. In this case it appears that the best fit density ρ_s is about 0.3 g/cm^3, and the initial preablation mass is about 1.9×10^{-4} g. Figure 4b is a similar set of plots but representing trace #10 (from Figure 3b). In this case the best fit ρ_s is again about 0.3 and the initial mass is about 2.7×10^{-4} g. We have made similar plots (not shown here) for each of the other measured traces, and we find that for the

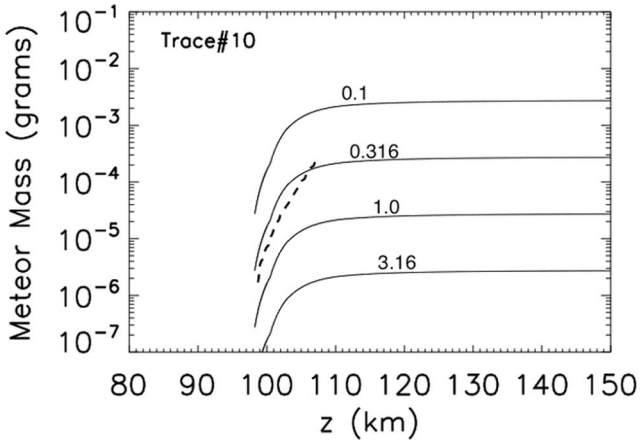

Figure 4b. Same as for Figure 4a but representing trace #10.

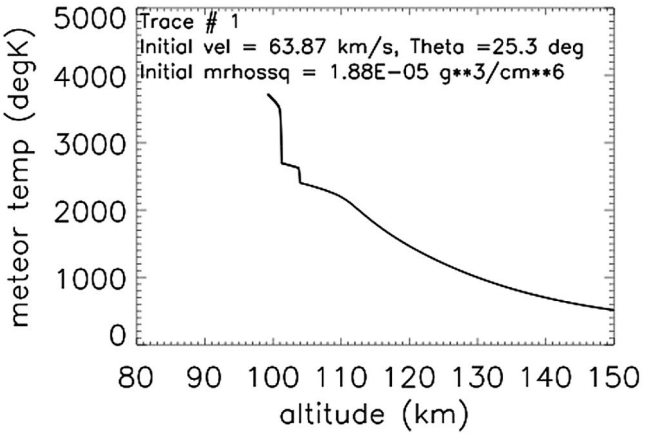

Figure 5a. Computed temperature history for the same meteor as in Figure 3a.

typical traces (altitudes between 95 and 110 km) the average best fit ρ_s is about 0.7. Not counting the anomalously high-altitude cases, the fitted values are 0.3, 1., 0.3, 0.5, 0.3, 1., 2., 0.3, 0.3, 0.3, 0.4, 0.2, 0.2, 0.2, 1., 0.3, 0.3, and 1. g/cm^3.

[24] It does not seem surprising that the ρ_s values obtained in this way show a large spread. However, the two unique higher-altitude traces (traces # 4 and 27, which span an altitude range between 112 and 125 km) are notable, in that the mass1 values (derived from the radar cross sections) are in the range 10^{-3} to 10^{-2} grams (notably much larger than those obtained for the lower-altitude cases), while the $m\rho_s^2$ values derived from the measured deceleration rates are unusually small. By the reasoning described above this would lead us to infer exceptionally small values of ρ_s, which seem not to be believable. This may be a subject for further study.

[25] To elaborate on some further details of the model computations: Figures 5a and 5b show more results from one of the runs, namely, the one representing trace #1. Figure 5a shows the computed meteoroid temperatures

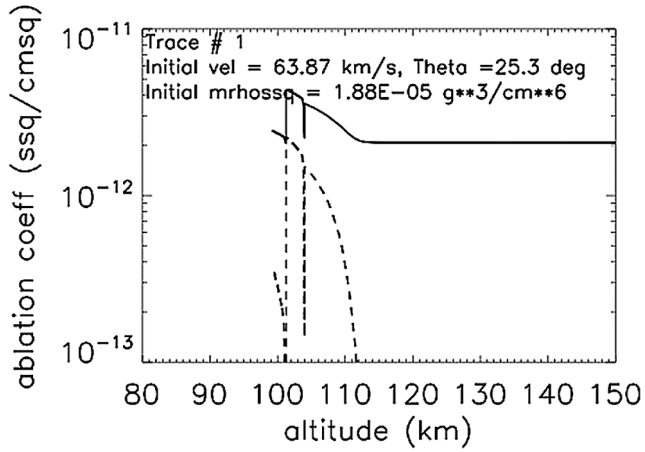

Figure 5b. Computed ablation coefficient versus altitude for the same meteor as in Figures 3a and 5a. The dashed curve is the evaporative contribution, and the solid curve is the total.

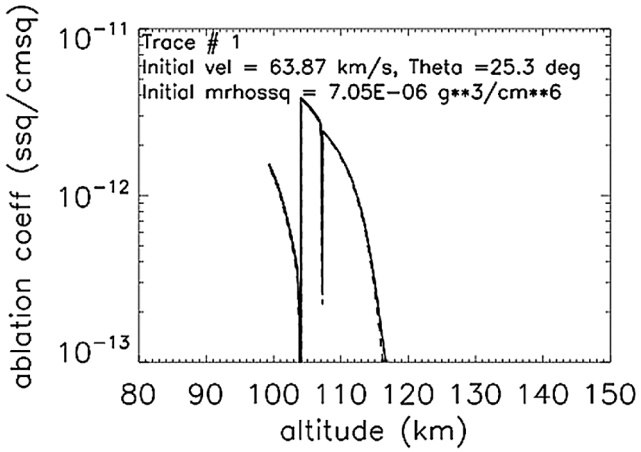

Figure 5c. Computed ablation coefficient versus altitude for the same case as in Figures 5a and 5b, when in the computation the assumed sputtering energy E* is raised to 1000 eV.

versus altitude, showing the successive evaporation of MgO, FeO and SiO_2; and Figure 5b shows the computed variations of the effective ablation coefficient σ with altitude, including the total σ and the separate evaporative contribution.

[26] For meteoroids composed of mixtures of materials the total vapor pressure at any point is the sum of the vapor pressures of the individual constituents, irrespective of their relative amounts. Then the evaporation rate for each component should be given by the Langmuir equation (equation (7)), irrespective of the fraction of that component in the mixture. Then, at each instant all of the constituents will be evaporating simultaneously at rates proportional to their individual vapor pressures until such times as each successive constituent disappears by evaporation. One result of this is that the temperature rises in a series of discrete steps, where the steps correspond to the disappearances of successive components. This is illustrated in Figure 5a. The ablation coefficients also exhibit a stepwise character, but with sharp decreases between successive steps, as is shown in Figure 5b. It is notable of course that the ablation coefficients are by no means constant, in contradiction to the trial assumption in equation (5).

[27] Our assumed sputtering contribution to the ablation coefficient produces a substantial difference in the computed ablation and deceleration rates. Figure 5c shows the computed ablation coefficient versus altitude for the same case as that shown in Figures 5a and 5b, but where in the computation the sputtering energy E* was raised to 1000 eV per molecule, so that the sputtering contribution to sigma was reduced to 3.1×10^{-14} s^2/cm^2. This value of E* would be in better agreement with the laboratory data. The result was a considerable reduction in the effective average ablation coefficients and a reduction in the meteoroid deceleration rates.

6. Direct Determination of $m\rho_s^2$ From the Deceleration Data

[28] The quantity $m\rho_s^2$ can be determined directly from the fitted velocity and deceleration rate data without the need to use the computer model, but assuming only that the meteoroid is a sphere. Then the rate of deceleration is as given by equation (3). For a sphere of density ρ_s the quantity πr^2 is $\pi r^2 = 1.209\ (m/\rho_s)^{2/3}$. Then, combining these two equations we obtain

$$m\rho_s^2 = \left[-1.209\ \rho\ v^2/(dv/dt)\right]^3. \qquad (11)$$

The values of $m\rho_s^2$ thus determined are of course very sensitive to errors in the measured/fitted deceleration rates. If we nevertheless proceed to evaluate the $m\rho_s^2$ from the data fits for 27 of the measured traces, and plot them as functions of altitude, the result is Figure 6. Only about twenty of these curves seem to be believable, namely, those that slope upward to the right and are concave downward. This set of twenty is the same as the twenty for which we found agreement between the computed and measured deceleration rates as described in the previous section.

[29] Despite the expected inaccuracies in these $m\rho_s^2$ values, it is of interest to compare them with the corresponding values that we determined in section 5 from fitting the model-computed decelerations to the data. Table 2 shows, for each of the 20 chosen traces, (1) the initial (uppermost) altitude, (2) the initial value of $m\rho_s^2$ at that altitude, as determined directly from the data using equation (11), (3) the $m\rho_s^2$ value at the same altitude as computed with the model, and (4) the value extrapolated to the top of the atmosphere using the model. As expected, the agreement between the values in columns 3 and 4 is not very good, but nor is it extremely bad in most cases.

[30] This procedure (i.e., using equation (11)) has the obvious advantage that it does not use any assumptions about the meteoroid composition, whereas in using the model a composition must be assumed. In both cases we assume a spherical shape. Using the model has the advantage that it allows us to extrapolate the $m\rho_s^2$ to the top of the atmosphere.

[31] Obviously, our quantity $m\rho_s^2$ is closely related to the familiar "ballistic parameter," $BP \equiv -\rho\ v^2/(dv/dt) = m / \pi\ r^2$. That is $m\rho_s^2 = 1.768\ (BP)^3$.

7. Discussion

[32] As noted in section 2, the meteoroid line-of-sight velocities were derived from third-order polynomial fits of

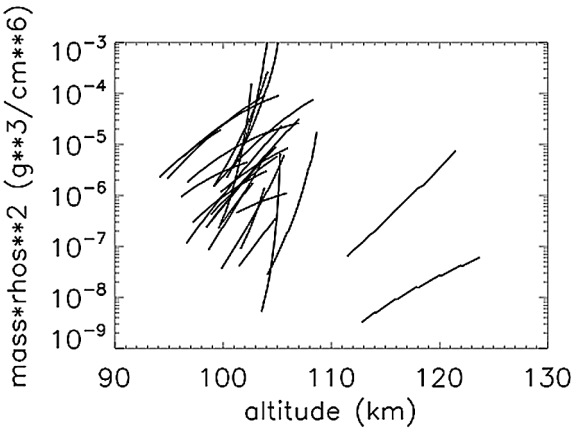

Figure 6. A composite plot of the combined variable $m\rho_s^2$ for 27 traces.

Table 2. Comparisons Between Values of $m\rho_s^2$ Determined Directly From the Data Via Equation (11) and Values Determined by the Method Described in Section 3

Trace #	Initial Altitude (z1) (km)	$m\rho_s^2$ at z1 From Equation (11)	$m\rho_s^2$ at z1 From Model	$m\rho_s^2$ (z = ∞) From Model
1	104	5.e-6	5.e-6	1.9e-5
4	124	6.e-8	2.0e-8	3.9e-8
6	104	2.5e-4	3.4e-5	6.2e-5
8	105	1.0e-4	2.4e-4	3.6e-4
9	108	7.e-5	3.e-5	4.3e-5
10	107	3.e-5	1.7e-5	2.7e-5
11	102	3.5e-6	5.e-5	2.6e-4
12	104	9.e-5	7.e-5	1.0e-4
13	104	4.e-6	9.e-6	2.3e-5
15	105	7.e-6	1.1e-5	2.6e-5
16	103	2.e-6	3.e-6	3.0e-5
17	105	2.5e-5	1.5e-5	3.0e-5
20	104	1.4e-6	1.0e-6	7.1e-6
23	105	4.e-7	8.e-7	5.0e-6
24	106	7.e-6	2.5e-6	8.1e-6
25	107	3.e-5	9.e-5	1.3e-4
27	122	9.e-6	1.8e-7	2.7e-7
28	106	1.0e-5	2.0e-5	3.6e-5
30	105	1.0e-5	7.e-6	1.4e-5
32	100	2.e-5	8.e-5	3.0e-4

the range versus time data, and converted to 3-D velocities by using the trajectory inclinations derived from the monopulse data. It has been encouraging to find that these 3-D velocities can be fitted so well as quadratic functions of Q. We generally find that the fitted velocities are within ±0.2% of the original ones. However, we still find that when we try to infer the $m\rho_s^2$ quantities directly from these data, as in section 6, that some of the $m\rho_s^2$ versus altitude curves curve the wrong way.

[33] We are currently in the process of analyzing a much larger set of ALTAIR meteor data from 2008, where with this data set the line-of-sight velocities are determined from measured Doppler frequency shifts of the reflected radar signals (R. Loveland et al., Comparison of methods of determining meteoroid range rates from LFM chirped pulses, submitted to *Radio Science*, 2010). As with the 1998 data the corresponding trajectory inclination angles are determined from the monopulse measurements of the instantaneous x, y and z positions. Using these inclination angles together with the known elevation angle of the radar beam, we then convert the measured line-of-sight velocities to 3-D velocities. It was to be hoped that these velocities might be more accurate than those described in the previous paragraph for the 1998 data set. However, present indications are that the accuracies are about the same, i.e., that the quadratic fits of 3-D velocity versus Q match the data to within ±0.2%.

[34] For purposes of evaluating the initial values of $m\rho_s^2$ we have chosen to use the computer model to find the values that produce the best fits to the deceleration rate data. However, a serious problem with that is that the model results are sensitive to the assumed chemical compositions of the meteors, which are of course not known. Our assumption of the olivine-like composition was convenient because the necessary data on vapor pressures and heats of sublimation of the decomposition products were available in the literature.

[35] In the process of comparing the model results to the deceleration data we found that the fits were improved when we assumed a rather large sputtering contribution to the effective ablation coefficients, namely, 2×10^{-12} s^2/cm^2. This value is significantly larger than values that have been determined in laboratory measurements of sputtering from energetic ion bombardment of solid target materials [*Behrisch*, 1981; *Bodhansky et al.*, 1980; *Lebedinets and Shushkova*, 1970; *Ratcliff et al.*, 1997; *Tielens et al.*, 1994]. However, with meteoroids entering the atmosphere the collision fluxes are much larger than in the laboratory experiments, and for most of the time the meteoroids are molten. Then the laboratory results may not be directly comparable.

[36] The model results show that the meteor temperatures almost invariably exceed the melting points before very much ablation occurs. Nevertheless, in our twenty selected cases the ablation and deceleration rates appear to vary smoothly, without obvious evidence of fragmentation. This seems quite surprising. However, in the remaining twelve cases the failure to fit our model may possibly be an indication of fragmentation. That failure could of course be due to other causes, including our possibly incorrect guesses as to the meteoroid composition.

[37] In our computer model we have assumed that the vapors emitted by the meteors are molecular rather than atomic. This seems to differ from the assumptions in the model described by *Vondrak et al.* [2008] and *Janches et al.* [2009]. In view of the fact that the dissociation energies of, for instance, SiO_2, MgO and FeO are very much larger than their sublimation energies, it seems unlikely that the evaporation products would be atomic. On the other hand, subsequent collisions of the evaporated molecules with background air molecules would certainly lead to dissociation and/or ionization.

[38] In all but two of our best fit cases we arrived at initial meteoroid $m\rho_s^2$ values in the range 10^{-6} to 10^{-4} g^3cm^{-6}. The remaining two of the traces were at altitudes between 110 and 125 km, appreciably higher than the rest, and they indicated $m\rho_s^2$ values in the 10^{-8} to 10^{-7} gram range.

[39] A quantity of most interest is the meteoroid mass range implied by the radar measurements, and by our analysis we determine not the masses, but rather $m\rho_s^2$. If the density ρ_s is known, then a value of $m\rho_s^2$ implies a value of m. If we assumed a nominal ρ_s value of 1.0 g/cm^3, then our $m\rho_s^2$ values would imply a top-of-atmosphere mass range between about 10^{-6} and 10^{-4} grams. On the other hand, if we used the average value of ρ_s that we arrived at in section 5, then our inferred m values would be about two times larger. Or, if we used the more commonly assumed ρ_s value of 3.0, then they would be nine times smaller.

[40] Meteor radar measurements and estimations of meteoroid masses from measured velocities have a long history dating back to *McKinley* [1961] and *Evans* [1966] (measurements from Millstone Hill) and extensive subsequent measurements at Arecibo, including *Zhou et al.* [1995], *Zhou and Kelley* [1997], *Mathews et al.* [1997], *Janches et al.* [2000], and *Mathews et al.* [2001]. Subsequent measurements at ALTAIR, with more dynamic mass estimates as well as scattering masses, are described by *Close et al.* [2002c, 2004, 2005]. Dynamic mass measurements together with computer model simulations are

described by *Bass et al.* [2008] and *Dyrud and Janches* [2008].

[41] This paper represents yet another attempt at determining meteoroid dynamical masses, or rather $m\rho_s^2$ products, by combining HPLA radar velocity measurements and results from computer simulations. The quality of the results depends on (1) the degree of accuracy of the 3-D velocity measurements, (2) the manner in which the deceleration rates are derived from the velocity data, and (3) the degree of validity of the computer model. With respect to item 1, the velocity data benefit from the unique capabilities of the ALTAIR radar facility for determining both line-of-sight velocities and 3-D locations, leading to 3-D velocities. Regarding item 2, the accuracy of the derived deceleration rates depends on the accuracy of the polynomial fits to the velocities, where in this study we have used least squares quadratic fits of the 3-D velocities versus Q (path integral of the air density). With respect to item 3, we think that our present model (and that of *Vondrak et al.* [2008]) are closer approximations to reality than most earlier models. However, a frequently stated problem with dynamical mass measurements is the need for assuming a value for the density ρ_s. In this paper we have attempted to determine ρ_s by combining our $m\rho_s^2$ values with m values determined from radar cross sections. The accuracy of these ρ_s values is only as good as the separate $m\rho_s^2$ or m values, or both in combination.

[42] It is to be noted that the dynamical mass values derived from our equation (11) will be eight times smaller than values derived from *Close et al.* [2005, equation 8], in which the quantity $A\gamma$ (meteor projected surface area times drag coefficient) was taken to be $2\pi r^2$, the value adopted previously by *Evans* [1966]. Our equation (11) avoids the concept of a drag coefficient, and takes the projected surface area A to be just πr^2. Then in the free molecular flow limit the rate of air molecule collisions on the surface is nvA per second, where n is the local air molecule number density; the momentum delivered per collision is $\mu_{air}v$, where μ_{air} is the air molecule mass, and we assume perfectly inelastic collisions. Then from Newton's second law $dv/dt = -\pi r^2 \rho v^2/m$ (our equation (3)). And since the mass of a sphere of density ρ_s is $(4/3)\pi r^3 \rho_s$, equation (11) follows.

[43] Our top-of-atmosphere mass range of 1×10^{-6} to 1×10^{-4} grams is in reasonable agreement with the 1×10^{-7} to 1×10^{-4} g range quoted by *Dyrud and Janches* [2008] based on Arecibo measurements combined with their computer model results. It is our opinion that dynamical mass determinations have been somewhat under-appreciated in the past [see also *Bass et al.*, 2008; *Close et al.*, 2007]. We think that the velocity and deceleration rate versus altitude curves in our Figures 1 and 2, and the $m\rho_s^2$ versus altitude plots in Figure 6 demonstrate that in the majority of our 32 cases the $m\rho_s^2$ values are reliable. The appropriate value (or values) for ρ_s is, however, still a matter for further study.

8. Summary

[44] It appears that with most of these 32 radar traces the range and altitude versus time measurements are of sufficient quality to allow us to extract reliable velocities, trajectory inclinations and deceleration rates. In about 80% of the cases the velocities can be fitted with good accuracy as quadratic functions of the integrals of the air densities along the measured trajectories, and the time derivatives of these functions provide reasonable values of the deceleration rates. We have used these fitted velocities and deceleration rates together with a computer model to determine best fit values of the initial $m\rho_s^2$, the product of the initial (top-of-atmosphere) meteoroid mass times its mass density squared, successfully in about 20 of the 32 cases. The model, which we have described, treats the coupled processes of deceleration through air molecule collisions and the associated heating of the meteor, together with cooling by blackbody emission and by evaporation of its constituents, and the rate of loss of mass through evaporation and by sputtering. We find that the meteoroids must invariably melt before much ablation occurs. Our fitting procedure does not provide information about the separate quantities m and ρ_s. However, separate estimates of the masses m have been obtained from the measured radar scattering cross sections, using the Close et al. electrostatic scattering model. By combining these m values with the $m\rho_s^2$ we have obtained values of ρ_s, all of which fall in the range between 0.2 to 3 g/cm^3, with an average of 0.7. We have also described a process by which we can obtain $m\rho_s^2$ values directly from the velocity and deceleration data without using the computer model, although the results are very sensitive to errors in the decelerations.

Appendix A: The Mathematical Model

A1. Definitions of Variables

[45] Index *i* refers to the *i*th chemical constituent.

Notation

t	time (s)
z	altitude (cm)
ρ_s	meteoroid mass density (g/cm^3)
r	meteoroid radius (assumed spherical)
M	meteoroid mass = $(4\pi/3)\rho_s r^3$
m_i	mass of the *i*th meteoroid constituent (g)
f_i	mass fraction of the *i*th constituent
v	meteoroid velocity (cm/s)
T	meteoroid temperature (assumed isothermal)
θ	trajectory zenith angle
$\rho(z)$	local air density (g/cm^3)
H	meteoroid total enthalpy (ergs)
$\Delta H_{vap(i)}$	heat of vaporization (erg/g) of the *i*th constituent
ΔH_{sput}	enthalpy loss by sputtering (ergs)
E^*_{sput}	energy required for sputtering of one gram (erg/g)
$\mu_{m(i)}$	molecular weight of the *i*th constituent (g/molec))
$\mu_{vap(i)}$	molecular weight of the *i*th vapor constituent (g/molec)
σ_{SB}	Stephan-Boltzmann constant (erg cm^{-2} deg^{-4} s^{-1})
C_p	specific heat of meteoroid material (erg/g)

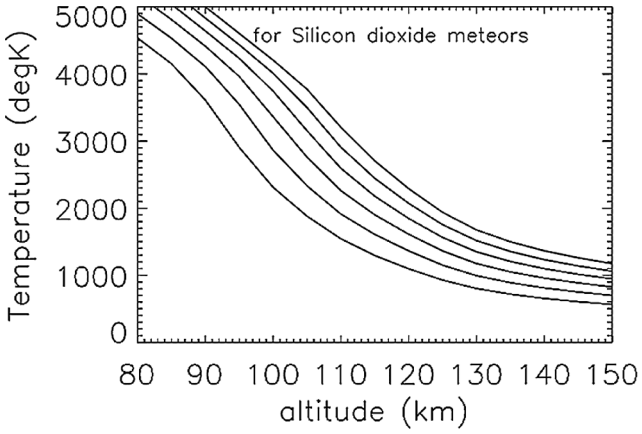

Figure B1a. Composite plots of steady state temperatures versus altitude for SiO_2 meteors with velocities of 30, 40, 50, 60, 70, and 80 km/s (in that order from bottom to top).

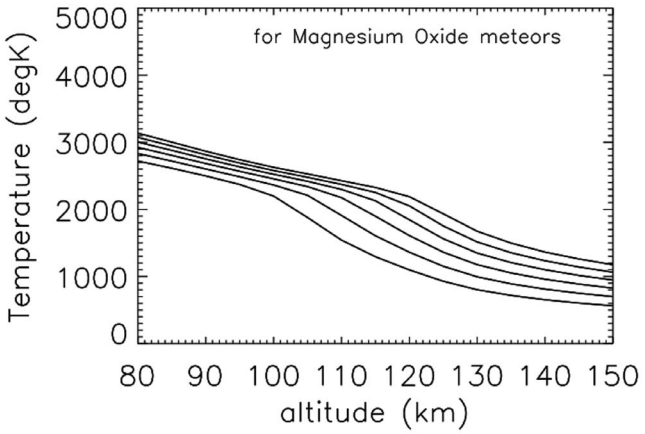

Figure B2a. Same as in Figures B1a and B1b but for magnesium oxide meteors.

$P_{vap(i)}$ vapor pressure of the *i*th constituent (d/cm^2)

$A_{vap(i)}$ and $C_{vap(i)}$ constants for the *i*th meteoroid constituent. Index *i* refers to the *i*th chemical constituent.

A2. Differential (and Other) Equations

Notation

$$M = \sum_i m_i$$
$$f_i = m_i/M$$
$$dz/dt = -v\cos\theta\ dt$$
$$dv/dt = -\pi r^2 \rho v^2/m$$
$$(dH/dt)_{coll} = 0.5\ \pi r^2 \rho v^3$$
$$dm_i/dt = (dm_i/dt)_{sput} + (dm_i/dt)_{evap}$$
$$(dm_i/dt)_{evap} = -4\pi r^2\ \mu_{vap(i)}\ \{3.51 \times 10^{+19}\ P_{vap(i)}/(\mu_{vap(i)}T)^{1/2}\}$$
(if $m_i > 0$. Otherwise zero)
$$(dm_i/dt)_{sput} = -f_i \mu_{m(i)} (dH/dt)_{coll}/E^*_{sput}$$
$$dH/dt = (dH/dt)_{coll} + (dH/dt)_{rad} + (dH/dt)_{evap}$$
$$(dH/dt)_{rad} = -4\pi r^2 \sigma_{SB} T^4$$
$$(dH/dt)_{evap} = \Sigma_i\ \Delta H_{vap(i)}\ (dm_i/dt)_{evap}$$
$$T = H/(C_p\ M)$$
$$P_{vap(i)} = A_{vap(i)} \exp(-C_{vap(i)}/T)$$

Appendix B: Meteor Temperatures and Evaporative Ablation, Quasi-analytic Solutions of the Steady State Equations, for a Single-Component Meteor

[46] Simple calculations show that an incoming meteor must be heated by air molecule collisions to quite high temperatures, which are mitigated by the emission of blackbody radiation and by evaporative cooling associated with Langmuir evaporation of the individual constituents. In the present case the meteoroids are quite small, so that heat conduction is fast enough to assure that their internal temperature profiles are isothermal. The collisional energy input rate is $\pi r^2 \rho v^3/2$. The radiative energy loss rate is $4\pi r^2 \sigma_{SB} T^4$, where T is the meteoroid temperature and σ_{SB}

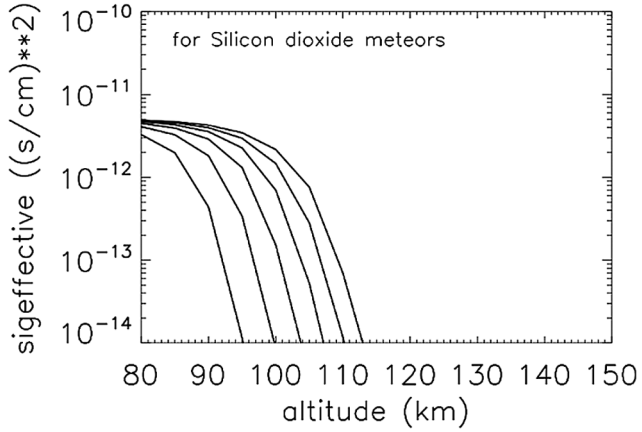

Figure B1b. Composite plots of effective ablation coefficients versus altitude for the same set of cases and in the same order.

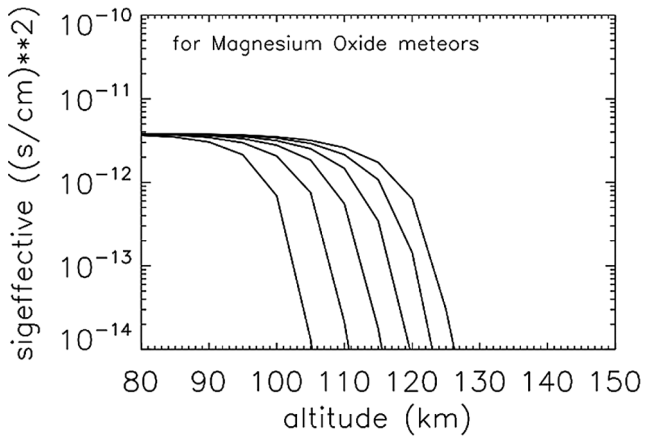

Figure B2b. Same as in Figures B1a and B1b but for magnesium oxide meteors.

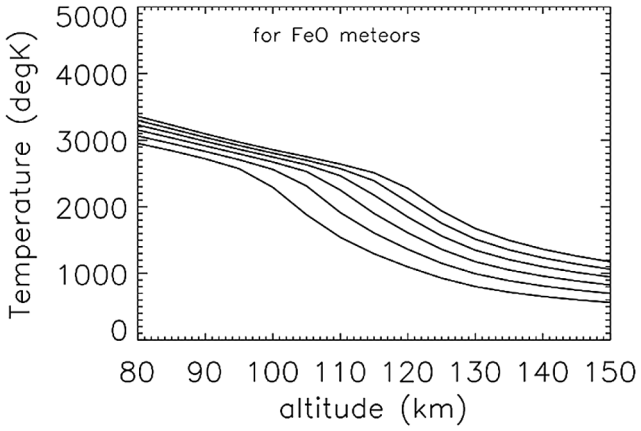

Figure B3a. Same as in Figures B1a and B1b but for ferrous oxide meteors.

is the Stephan-Boltzmann constant. The vapor pressure for a single molecular constituent is approximated by the Clapeyron-Claussius relation

$$P_{vap} = A \exp(-C/T), \tag{B1}$$

where A and C are constants characteristic of the particular evaporating meteor constituent. And the evaporative flux from the surface is given by the Langmuir relation [*Taylor and Langmuir*, 1933]

$$F_{evap} = C_{flx}\ P_{vap}/\left(\mu_{vap} T\right)^{1/2} cm^{-2} s^{-1}, \tag{B2}$$

where μ_{vap} is the molecular weight of the vapor. If P_{vap} is in dynes/cm^2 and μ_{vap} is in grams, then the constant C_{flx} is equal to 3.40×10^7. Then the rate of energy loss from the meteor surface due to evaporation is $4\pi r^2\ \Delta H_{sblm}\ F_{evap}$, where ΔH_{sblm} is the heat of sublimation (erg/molecule). We expect that the collisional heating and the radiative and evaporative cooling will balance each other, so that at each point in the meteoroid trajectory the temperature should be given by the steady state relation

$$\pi r^2 \rho v^3/2 - 4\pi r^2 \sigma_{SB} T^4 - 4\pi r^2\ \Delta H_{sblm}\ F_{evap} = 0. \tag{B3}$$

(Equation (B3) is equivalent to *Hunt et al.* [2004, equation 3] or *Vondrak et al.* [2008, equation 2], although we assume the steady state condition dT/dt = 0 (or negligible).)

[47] This equation can be solved for T by Newton-Raphson iteration, and when T is determined we can calculate the evaporative mass loss rate

$$dm/dt = -4\pi r^2\ \mu_{vap}\ F_{evap} \tag{B4}$$

at each point along the trajectory. Then using equation (B4) together with equation (2) we can solve for the evaporative contribution to the effective ablation coefficient σ, which is now a function of altitude. From equations (B3) and (B4) we can see that this effective σ is a function of the air density ρ, the velocity v and the thermodynamic properties of the meteor material (or individual meteor constituents), but it is not directly dependent on the meteoroid mass or the mass density or the trajectory inclination angle.

[48] Figures B1a and B1b, Figures B2a and B2b, and Figures B3a and B3b show computed temperatures and effective ablation coefficients as functions of altitude for meteoroids composed of pure SiO_2, MgO, or FeO, respectively. These three compounds are expected to be the decomposition products of the mineral olivine, which is commonly found to be a dominant constituent in stony meteorites (Chemical composition of meteorites data available at http://meteorites.wustl.edu/metcomp/index.htm).

[49] It is interesting to note that in Figures B1b, B2b, and B3b in each case the effective sigmas tend to converge to a common value at the lowest altitudes. This is due to the fact that at the lowest altitudes the temperatures are so high that the evaporative cooling rate dominates over the radiative cooling rate. Then the second term in equation (B3) can be ignored in comparison with the third, and combining equations (B3), (B4), and (2) gives

$$\sigma = \mu_{vap}/(2\Delta H_{sblm}), \tag{B5}$$

(limit for low altitudes and high temperatures).

[50] It is also interesting that the limiting low-altitude values of the effective sigmas are not very different from the average σ values that we determined from our data using the constant σ assumption and equation (5) (although the details of that analysis will not be shown).

[51] In writing equations (B3) and (B4) we have not mentioned the fact that the meteoroids can be expected to melt before they vaporize to an appreciable extent. The present radar data seem to indicate that the meteoroids do not immediately disintegrate upon melting; that is, the traces seem to be continuous when the temperatures are expected to exceed the melting points. Apparently the molten meteoroids are held together by surface tension. In writing equation (B3) we have not specifically included the solid-liquid transition, and we have used the heat of sublimation ΔH_{sblm} as if the meteoroid evaporated directly from the solid phase.

[52] The calculations in this section have been for hypothetical meteoroids composed of a single vaporizable material. Of course actual meteors are expected to be made of a mixture of materials, each of which would vaporize at its own rate. More detailed computations including mixtures of

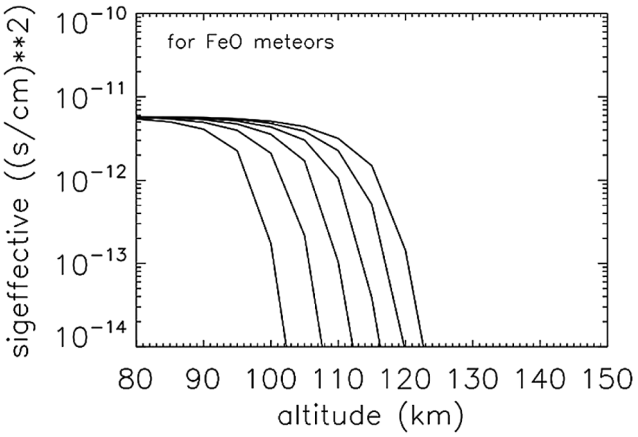

Figure B3b. Same as in Figures B1a and B1b but for ferrous oxide meteors.

materials have been described in section 4. In the present section we have also ignored the effect of sputtering. It is to be expected that at the highest altitudes, where the meteoroid temperatures are relatively low, the mass loss rate will be dominated by sputtering, so the effective σ should include an added constant term for the sputtering contribution. On the basis of laboratory experimental results and theoretical studies [*Behrisch*, 1981; *Bodhansky et al.*, 1980; *Lebedinets and Shushkova*, 1970; *Ratcliff et al.*, 1997; *Rogers et al.*, 2005; *Tielens et al.*, 1994], we would expect that the sputtering term should be of the order of 4×10^{-14} s^2/cm^2. However, our deceleration data suggest a much larger value, of order 2×10^{-12}. The laboratory sputtering measurements of course involved much lower collisional fluxes than those expected for an incoming meteor, and much lower temperatures, and solid rather than molten or fragile targets.

[53] The low values of density and the high rate of sputtering are consistent with meteoroids that are very fine-grained and loosely assembled, consistent with the meteoroids originating from (long period and Halley-type) comets, as in the model by *Nesvorny et al.* [2010].

[54] The physicochemical parameters used in these calculations have been shown in Table 1.

Appendix C: The Electrostatic Scattering Model

[55] The electrostatic scattering model is described in detail by *Close et al.* [2004, 2005] [see also *Dyrud et al.*, 2005] and will be discussed only briefly here. It is based on assumptions that (1) the electron cloud surrounding the meteoroid can be approximated as spherically symmetric and (2) the electron distribution within the cloud is a Gaussian in r, given by

$$n_e = n_{max} \exp\left[-(r/r_{max})^2\right].$$

A theoretical analysis is developed for the scattering of a radar beam from a spherical plasma distribution, through which for each echo along a trace the parameters n_{max} and r_{max} can be determined from a fit to the measured scattering cross section. After the n_{max} and r_{max} are determined, the areal integrals $q = 2\pi \int_0^{r_{max}} n_e\, r\, dr$ ("line densities") are formed for all the points along a trace. Then the total number of electrons along a trace is $N_e = \int q\, ds = \int q\, v\, dt$. Then assuming that the ionization efficiency β is as given by the expression due to *Jones* [1997] the meteoroid mass is determined from $m = N_e\, \mu/\beta$, where μ is the average weight of the meteoroid atom.

[56] The scattering model is validated rather well by the observed fact that for thirty individual meteoroid traces recorded at the separate UHF and VHF radar frequencies at the loci of maximum scattering cross section the values of the parameters r_{max} and n_{max} are in close agreement. Nevertheless, it is clear that several of the model assumptions are debatable. We are currently in the process of developing a hybrid Monte Carlo theoretical model that is designed to compute the plasma distribution in two dimensions surrounding the meteoroid. Preliminary results indicate that the distribution is far from spherical, being quite compressed in front of the meteoroid and extending to considerable distances in the wake.

[57] **Acknowledgments.** Masaki Fujimoto thanks Peter Jenniskens, Stanley Briczinski, and another reviewer for their assistance in evaluating this paper.

References

Akopov, F. A. (1999), Behavior of zirconium dioxide ceramic under the operating conditions of an external trap, *At. Energy*, *87*, 505–509, doi:10.1007/BF02673209.

Bass, E., M. Oppenheim, J. Chau, and A. Olmstead (2008), Improving the accuracy of meteoroid mass estimates from head echo deceleration, *Earth Moon Planets*, *102*, 379–382, doi:10.1007/s11038-007-9202-2.

Behrisch, R. (Ed.) (1981), Topics in applied physics, in *Sputtering by Particle Bombardment*, Springer, Berlin.

Bodhansky, J., J. Roth, and H. L. Bay (1980), An analytical formula and important parameters for low-energy ion sputtering, *J. Appl. Phys.*, *51*, 2861–2865, doi:10.1063/1.327954.

Brewer, L., and R. F. Porter (1954), A thermodynamic and spectroscopic study of gaseous magnesium oxide, *J. Chem. Phys.*, *22*, 1867, doi:10.1063/1.1739934.

Brewer, L., P. W. Giles, and F. R. Jenkins (1948), The vapor pressure and heat of sublimation of graphite, *J. Chem. Phys.*, *16*, 797, doi:10.1063/1.1746999.

Bronshten, V. A. (1983), *Physics of Meteor Phenomena*, Reidel, Dordrecht, Neth.

Ceplecha, Z., J. Borovicka, W. G. Elford, D. O. Revelle, R. L. Hawkins, V. Porubcan, and M. Simek (1998), Meteor phenomena and bodies, *Space Sci. Rev.*, *84*, 327–471, doi:10.1023/A:1005069928850.

Clarke, J. T., and B. R. Fox (1969), Rate and heat of vaporization of graphite above 3000 K, *J. Chem. Phys.*, *51*, 3231–3240, doi:10.1063/1.1672500.

Close, S., S. M. Hunt, M. J. Minardi, and F. M. McKeen (2000), Analysis of perseid meteor head-echo data collected using the Advanced Research Projects Agency Long-Range Tracking and Instrumentation Radar (ALTAIR), *Radio Sci.*, *35*, 1233–1240, doi:10.1029/1999RS002277.

Close, S., S. M. Hunt, F. M. McKeen, and M. J. Minardi (2002a), Characterization of Leonid meteor head echo data collected using the VHF-UHF Advanced Research Projects Agency Long-Range Tracking and Instrumentation Radar (ALTAIR), *Radio Sci.*, *37*(1), 1009, doi:10.1029/2000RS002602.

Close, S., M. Oppenheim, S. Hunt, and L. Dyrud (2002b), Scattering characteristics of high-resolution meteor head echoes detected and multiple frequencies, *J. Geophys. Res.*, *107*(A10), 1295, doi:10.1029/2002JA009253.

Close, S., M. Oppenheim, S. Hunt, F. McKeen, and A. Coster (2002c), Meteoroid mass determination using head echoes detected at multiple frequencies, in *Proceedings of Asteroids, Comets, Meteors-ACM 2002*, edited by B. Warmbein, *Eur. Space Agency Spec. Publ.*, *ESA SP-500*, 153–156.

Close, S., M. Oppenheim, S. Hunt, and A. Coster (2004), A technique for calculating meteor plasma density and meteoroid mass from radar head echo scattering, *Icarus*, *168*, 43–52, doi:10.1016/j.icarus.2003.11.018.

Close, S., M. Oppenheim, D. Durand, and L. Dyrud (2005), A new method for determining meteoroid mass from head echo data, *J. Geophys. Res.*, *110*, A09308, doi:10.1029/2004JA010950.

Close, S., P. Brown, M. Campbell-Brown, M. Oppenheim, and P. Colestock (2007), Meteor head echo radar data: Mass-velocity selection effects, *Icarus*, *186*, 547–556, doi:10.1016/j.icarus.2006.09.007.

Dyrud, L. P., and D. Janches (2008), Modeling the head echo using Arecibo radar observations, *J. Atmos. Sol. Terr. Phys.*, *70*, 1621–1632, doi:10.1016/j.jastp.2008.06.016.

Dyrud, L. P., L. Ray, M. Oppenheim, S. Close, and K. Denney (2005), Modelling high-power large-aperture meteor trails, *J. Atmos. Sol. Terr. Phys.*, *67*, 1171–1177, doi:10.1016/j.jastp.2005.06.016.

Evans, J. V. (1966), Radar observations of meteor deceleration, *J. Geophys. Res.*, *71*, 171–188.

Fabian, R. (1993), *Vacuum Technology: Practical Heat Treating and Brazing*, 253 pp., ASM Int., Materials Park, Ohio.

Ferguson, F. R., J. A. Nuth III, and N. M. Johnson (2004), Thermogravimetric measurement of the vapor pressure of iron from 1573 K to 1973 K, *J. Chem. Eng. Data*, *49*, 497–501, doi:10.1021/je034152w.

Hunt, S. M., M. Oppenheim, S. Close, P. G. Brown, F. McKeen, and M. Minardi (2004), Determination of meteoroid velocity distribution at the Earth using high-gain radar, *Icarus*, *168*, 34–42, doi:10.1016/j.icarus.2003.08.006.

Janches, D., L. P. Dyrud, S. L. Broadley, and J. M. C. Plane (2009), First observation of micrometeoroid differential ablation in the atmosphere, *Geophys. Res. Lett.*, *36*, L06101, doi:10.1029/2009GL037389.

Janches, D., J. D. Mathews, D. D. Meisel, and Q. H. Zhou (2000), Micrometeor observations using the Arecibo 430 MHz radar, *Icarus*, *145*, 45–63.

Jones, W. (1997), Theoretical and observational determination of the ionization coefficient of meteors, *Mon. Not. R. Astron. Soc.*, *288*, 995–1003.

Lebedinets, V. N. (1973), Evolutionary and physical properties of meteoroids, in *Proceedings of the International Astronomical Union*'s *Colloquium 13*, vol. 319, edited by C. L. Hemenway, P. M. Millman, and A. F. Cook, p. 259, NASA, Albany, N. Y.

Lebedinets, V. N., and V. B. Shushkova (1970), Micrometeorite sputtering in the ionosphere, *Planet. Space Sci.*, *18*, 1653–1659, doi:10.1016/0032-0633(70)90039-5.

Mathews, J. D., D. D. Meisel, K. P. Hunter, V. S. Getman, and Q. Zhou (1997), Very high resolution studies of micrometeors using the Arecibo 430 MHz radar, *Icarus*, *126*, 157–169, doi:10.1006/icar.1996.5641.

Mathews, J. D., D. Janches, D. D. Meisel, and Q.-H. Zhou (2001), The micrometeoroid mass flux into the upper atmosphere: Arecibo results and a comparison with prior estimates, *Geophys. Res. Lett.*, *28*, 1929–1932, doi:10.1029/2000GL012621.

McKinley, D. W. R. (1961), *Meteor Science and Engineering*, McGraw Hill, New York.

Nesvorny, D., P. Jenniskens, H. F. Levison, W. F. Bottke, D. Vokrouhlicky, and M. Gounelle (2010), Cometary origin of the zodiacal cloud and carbonaceous micrometeorites. Implications for hot debris disks, *Astrophys. J.*, *713*, 816–836, doi:10.1088/0004-637X/713/2/816.

Opik, E. J. (1958), *Physics of Meteor Flight in the Atmosphere*, Interscience, New York.

Patnaik, P. (2002), *Handbook of Inorganic Chemicals*, McGraw-Hill, New York.

Pecina, P., and Z. Ceplecha (1983), New aspects in single-body meteor physics, *Bull. Astron. Inst. Czechosl.*, *34*, 102–121.

Ratcliff, P. R., M. J. Burchell, M. J. Cole, T. W. Murphy, and F. Allahdadi (1997), Experimental measurements of hypervelocity impact plasma yield and energetics, *Int. J. Impact Eng.*, *20*, 663–674, doi:10.1016/S0734-743X(97)87453-2.

Rogers, L. A., K. A. Hill, and R. L. Hawkes (2005), Mass loss due to sputtering and thermal processes in meteoroid ablation, *Planet. Space Sci.*, *53*, 1341–1354, doi:10.1016/j.pss.2005.07.002.

Taylor, J. B., and I. Langmuir (1933), The rates of evaporation of atoms, ions and electrons from caesium films on tungsten, *Phys. Rev.*, *44*, 423–458, doi:10.1103/PhysRev.44.423.

Tielens, A. G. G. M., C. F. McKee, C. G. Seab, and D. J. Hollenbach (1994), The physics of grain-grain collisions and gas-grain sputtering in interstellar shocks, *Astrophys. J.*, *431*, 321–340, doi:10.1086/174488.

Vondrak, T., J. M. C. Plane, S. Broadley, and D. Janches (2008), A chemical model of meteor ablation, *Atmos. Chem. Phys. Discuss.*, *8*, 14,557–14,606, doi:10.5194/acpd-8-14557-2008.

Wickramasinghe, N. C., and K. S. Krishna Swamy (1968), Comments on the possibility of interstellar quartz grains, *Astrophys. J.*, *154*, 397–400, doi:10.1086/149767.

Zhou, Q., C. A. Tepley, and M. P. Sulzer (1995), Meteor observations by the Arecibo 430 MHz incoherent scatter radar-I. Results from time-integrated observations, *J. Atmos. Terr. Phys.*, *57*, 421–431, doi:10.1016/0021-9169(94)E0011-B.

Zhou, Q. H., and M. C. Kelley (1997), Meteor observations by the Arecibo 430 MHz incoherent scatter radar. II. Results from time-resolved observations, *J. Atmos. Sol. Terr. Phys.*, *59*, 739–752, doi:10.1016/S1364-6826(96)00103-4.

S. Close, Department of Aeronautics and Astronautics, Stanford University, Stanford, CA 94305, USA.

P. L. Colestock, R. Loveland, and J. Zinn, Los Alamos National Laboratory, Mail Stop D436, Los Alamos, NM 87545, USA. (jzinn@lanl.gov)

A. MacDonell, Department of Astronomy, Boston University, Boston, MA 02215, USA.